Paper AAS 03-514

Parking Orbits for Human Missions to Mars

Damon F. Landau & James M. Longuski

School of Aeronautics and Astronautics
Purdue University
West Lafayette, Indiana

Paul A. Penzo

Global Aerospace Corporation
Altadena, CA

AAS/AIAA Astrodynamics Specialists Conference

Big Sky, Montana **August 3-7, 2003**

AAS Publications Office, P.O. Box 28130, San Diego, CA 92198

AAS 03-514

PARKING ORBITS FOR HUMAN MISSIONS TO MARS*

Damon F. Landau,† James M. Longuski,‡ and Paul A. Penzo§

Several Mars human-mission scenarios incorporate a parking orbit at either Earth or Mars. In many cases the parking orbit is not conveniently oriented with respect to the interplanetary leg (e.g., returning to Earth from a parking orbit at Mars). A method to reorient the spacecraft's orbit about a planet for a roundtrip mission is described. We also account for orbital precession effects during the parking orbit. We find that reorienting the parking orbit prior to departure can significantly reduce the total ΔV for many proposed missions.

INTRODUCTION

In many Mars mission designs, a vehicle is placed in a parking orbit. Generally, the orbit has the lowest periapsis and highest apoapsis practical to minimize the insertion and departure ΔV. Parking orbits reduce propulsion requirements because a smaller vehicle may then ferry the cargo and crew to and from the surface. A prime example is NASA's Design Reference Mission,[1] where the Earth Return Vehicle is placed in a highly elliptical Martian orbit. There are several other proposals that use parking orbits at Mars,[2,3] and some that incorporate parking orbits at both Earth and Mars.[4,5] To analyze the feasibility or effectiveness of the desired mission, we must estimate the ΔV cost of both placing the vehicle into the parking orbit and injecting to escape for the return trip. Often this cost is calculated as the sum of tangential burns at a common periapsis of the incoming/outgoing hyperbolic trajectory and the parking orbit (as in Case 1, Figure 1). However, this model does not account for the actual geometry of the transfer (as in Case 2, Figure 1) nor does it account for orbital precession due to perturbing forces. Ignoring these effects will underestimate the departure mass at low-Earth orbit, sometimes by up to 50%.[6,7]

The only case where no additional mass is required is when the orbit precesses at exactly the right rate to align the orbit for a tangential periapsis burn at departure. This case, however, is rare,[8,9] and often requires unacceptable transfer times and V_∞. An effective method of reorienting a parking orbit to allow tangential maneuvers at periapsis for the general case was introduced by Luidens and Miller in 1966.[10] Their method

† Graduate Student, School of Aeronautics and Astronautics, Purdue University, West Lafayette, IN 47907-2023, Member AAS, Student Member AIAA.

‡ Professor, School of Aeronautics and Astronautics, Purdue University, West Lafayette, IN 47907-2023, Member AAS, Associate Fellow AIAA.

§ Senior Engineer, Global Aerospace Corporation, 711 Woodbury Road, Suite H, Altadena, CA 91001-5327, Member AAS, Associate Fellow AIAA.

involves rotating, or twisting, the parking orbit about the line of apsides via a maneuver at apoapsis, and was thus termed the "apo-twist." This maneuver, as we shall see, requires the alignment of the major axes, which is accomplished here by placing no constraints on the inclinations of the parking orbits at the times of arrival and departure. We present this method as an ideal component of interplanetary mission design, and we extend the previous work to account for orbital precession. Performance characteristics are presented for several current Mars mission proposals.

The Problem

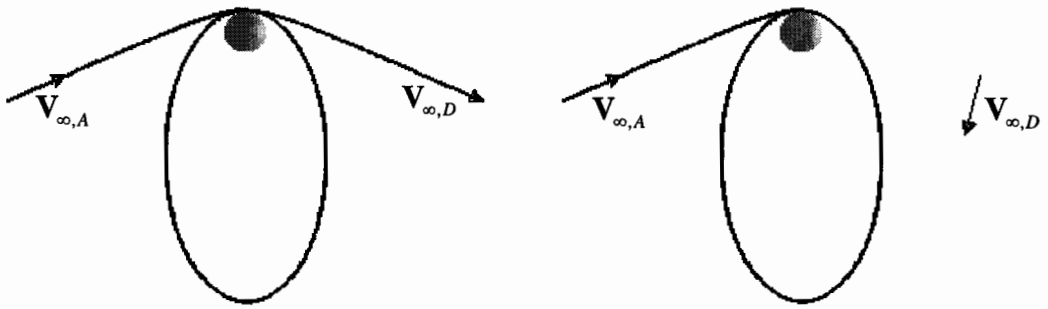

Case 1 Case 2

Figure 1 Orientation of Required $\mathbf{V}_\infty$ and Parking Orbit.

Case 1 presents no difficulties because the planet provides sufficient bending to reach $\mathbf{V}_{\infty,D}$ with a tangential burn at periapsis. Here, the approach hyperbola, parking orbit, and departure hyperbola are coplanar and have the same periapsis. To calculate the ΔV (assuming conic trajectories) only the magnitudes of $\mathbf{V}_{\infty,A}$ and $\mathbf{V}_{\infty,D}$ are needed: the cost of entering the parking orbit is found explicitly via Eq. (1),

$$\Delta V = \sqrt{V_{\infty,A}^2 + 2\mu/r_p} - \sqrt{\mu\left(2/r_p - 1/a\right)} \tag{1}$$

where μ is the gravitational parameter of the planet, r_p is the radius of periapsis, and a is the semi-major axis of the parking orbit. The cost of departing is found by replacing $V_{\infty,A}$ with $V_{\infty,D}$.

To achieve $\mathbf{V}_{\infty,D}$ in Case 2 seems difficult, but is possible with the apo-twist maneuver. In this case, $\mathbf{V}_{\infty,A}$, $\mathbf{V}_{\infty,D}$, and the parking orbit do not necessarily lie in the same plane. The approach, parking orbit, and departure trajectories can still share a common periapsis with the apo-twist, though this is not the case with several other methods. Since the direction of $\mathbf{V}_{\infty,D}$ is now critical, the total ΔV will be greater than that provided by Eq. (1).

Proposed Method

If the parking orbit must be reoriented, then an ideal place to perform the reorientation maneuver is apoapsis. This is simply because the velocity of the spacecraft

is lowest at this point, and therefore relatively easy to change (i.e. with low ΔV), especially for highly eccentric obits. To maintain its size and shape (a and e), the parking orbit is rotated along the line of apsides, i.e. the arrival and departure parking orbits share a common periapsis and apoapsis. The greatest possible twist angle with the apo-twist is 180°, which can be achieved by a ΔV that is exactly twice the apoapsis velocity. For a fixed periapsis, as the period of the orbit increases, the magnitude of the apo-twist maneuver decreases.

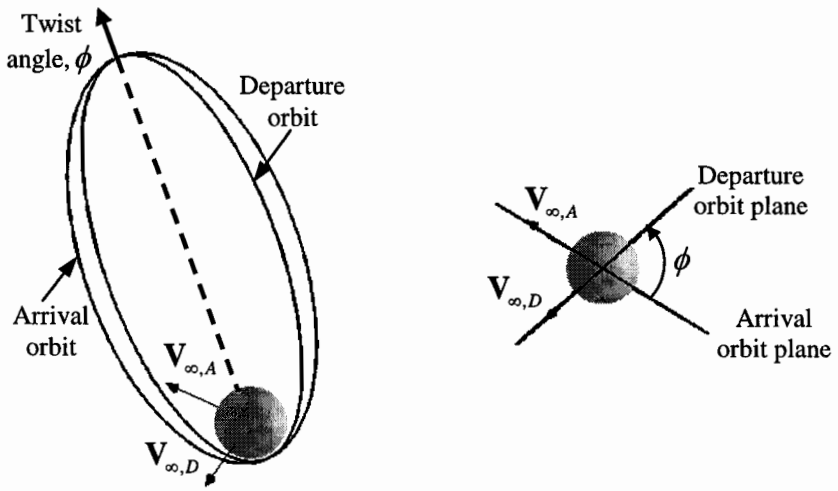

Figure 2 Rotation of Parking Orbit About Line of Apsides by Twist Angle ϕ. The Left Figure is a 3-D View and the Right Figure Shows the View Along the Line of Apsides.

DERIVATION OF EQUATIONS

No Perturbation Model: Analytic Solution

Since the parking orbit and approach hyperbola share a common periapsis, the periapsis vector is readily computed by specifying the right ascension (α) and declination (δ) of the V_∞ vector, the hyperbolic half-angle (A), and the B-plane angle (β). The interplanetary trajectory specifies the arrival and departure V_∞ vectors, while the V_∞ and desired periapsis magnitudes provide the hyperbolic half-angle [Eq. (1)], leaving the arrival and departure B-plane angles as free variables to choose the periapsis vector.

$$A = \sin^{-1}\left(\frac{\mu}{\mu + \mathrm{V}_\infty^2 r_p}\right); A \in [0°, 90°] \tag{2}$$

The B-plane angle targets the location around the disc of the planet for the spacecraft to aim. In Figure 3 the view direction is along the V_∞ vector (i.e. this vector is perpendicular to the view plane). The $\hat{\mathrm{z}}$ axis is rotated out of the view plane forward or backward through the declination, but both $\mathbf{T}$ and $\mathbf{B}$ (the aim point) are in the view plane. The B-plane angle is the angle between $\mathbf{T}$ and $\mathbf{B}$.

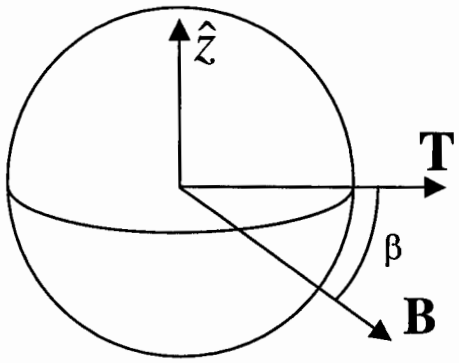

Figure 3 Diagram of B-Plane Angle (β). Note: $\mathbf{T} = \mathbf{V}_\infty \times \hat{\mathbf{z}}$, B is the Aim Point.

We calculate the orbital coordinate system ($\hat{r}, \hat{\theta}, \hat{h}$) at periapsis through sequential rotations of α, δ, β, and A, defining the direction cosine matrix from orbital coordinates to inertial coordinates ($\hat{x}, \hat{y}, \hat{z}$).

$$\begin{array}{c|ccc} & \hat{r} & \hat{\theta} & \hat{h} \\ \hat{x} & c_\alpha c_\delta s_A + (s_\alpha c_\beta + c_\alpha s_\delta s_\beta) c_A & c_\alpha c_\delta c_A - (s_\alpha c_\beta + c_\alpha s_\delta s_\beta) s_A & s_\alpha s_\beta - c_\alpha s_\delta c_\beta \\ \hat{y} & s_\alpha c_\delta s_A + (-c_\alpha c_\beta + s_\alpha s_\delta s_\beta) c_A & s_\alpha c_\delta c_A + (c_\alpha c_\beta - s_\alpha s_\delta s_\beta) s_A & -c_\alpha s_\beta - s_\alpha s_\delta c_\beta \\ \hat{z} & s_\delta s_A - c_\delta s_\beta c_A & s_\delta c_A + c_\delta s_\beta s_A & c_\delta c_\beta \end{array} \tag{3}$$

For the departure periapsis A = -A.

To simplify the analysis of this matrix, we define $\hat{z}$ to be perpendicular to the plane created by the incoming and outgoing $\mathbf{V}_\infty$ vectors (δ=0), and the incoming $\mathbf{V}_\infty$ right ascension is rotated to zero. This may be done because, for now, no perturbations are modeled and the planet's orientation is not critical. These assumptions provide the following conditions:

Arrival:

$$\alpha=0,\ \delta=0,\ A = A_A,\ \beta=\beta_A \tag{4}$$

Departure:

$$\alpha=\alpha',\ \delta=0,\ A = -A_D,\ \beta=\beta_D \tag{5}$$

Where α' is the angle (between 0° and 180°) from $\mathbf{V}_{\infty,A}$ to $\mathbf{V}_{\infty,D}$. The size and shape of the parking orbit provides the magnitude of periapsis, while the first column of (3) gives the direction of periapsis in inertial coordinates. Thus for the arrival and departure orbits to share a common periapsis ($\mathbf{r}_{p,A} = \mathbf{r}_{p,D}$), the following conditions [from the first column of (3)] must be satisfied.

$$s_{A_A} = -c_{\alpha'} s_{A_D} + s_{\alpha'} c_{\beta_D} c_{A_D} \tag{6}$$

$$c_{\beta_A} c_{A_A} = s_{\alpha'} s_{A_D} + c_{\alpha'} c_{\beta_D} c_{A_D} \tag{7}$$

$$s_{\beta_A} c_{A_A} = s_{\beta_D} c_{A_D} \tag{8}$$

We obtain Eq. (9) by solving (6) for $\cos\beta_D$. We then substitute Eq. (9) into Eq. (7) to get $\cos\beta_A$ [Eq. (10)]. The positive or negative value for β_2 may be chosen arbitrarily, but from (8), if β_A is positive then β_D must also be positive and vice versa.

$$c_{\beta_D} = \frac{s_{A_A} + c_{\alpha'} s_{A_D}}{s_{\alpha'} c_{A_D}} \tag{9}$$

$$c_{\beta_A} = \frac{s_{A_D} + c_{\alpha'} s_{A_A}}{s_{\alpha'} c_{A_A}} \tag{10}$$

This combination of B-plane angles will ensure that the incoming and outgoing V_∞ vectors may be achieved from the same periapsis and an orbital maneuver is required only at apoapsis.

The angle through which the orbit must rotate is the angle between the two angular momentum vectors, given by the third column of (3) and reproduced in Eq. (11). This angle (ϕ) is found by taking the dot product between the two angular momentum vectors [Eq. (12)].

$$\hat{h}_A = \begin{bmatrix} 0 \\ -s_{\beta_A} \\ c_{\beta_A} \end{bmatrix}, \hat{h}_D = \begin{bmatrix} s_{\alpha'} s_{\beta_D} \\ -c_{\alpha'} s_{\beta_D} \\ c_{\beta_D} \end{bmatrix} \tag{11}$$

$$c_\phi = \hat{h}_A \cdot \hat{h}_D = \frac{c_{\alpha'} + s_{A_A} s_{A_D}}{c_{A_A} c_{A_D}} \tag{12}$$

We find the reorientation cost for an impulsive burn via Eq. (13).

$$\Delta V = 2V_{apo} \sin(\phi/2) \tag{13}$$

This is simply the ΔV for rotating a vector ($\mathbf{V}_{apo}$) through a given angle (ϕ). Thus, for a given set of $\alpha', A_A, \& A_D$, the location of the apo-twist maneuver is calculated via Eqs. (9) and (10), and the cost is provided by Eq. (13).

In general, there will be two possible locations to perform the apo-twist [principal and non-principal values of (9) and (10)]. Geometrically, this occurs because the set of arrival and departure periapses form circles that rest on a sphere with a radius equal to the periapsis magnitude (see Figure 4). The intersections of these circles are locations where the arrival and departure parking orbits chare common apses, thus an apo-twist is possible.

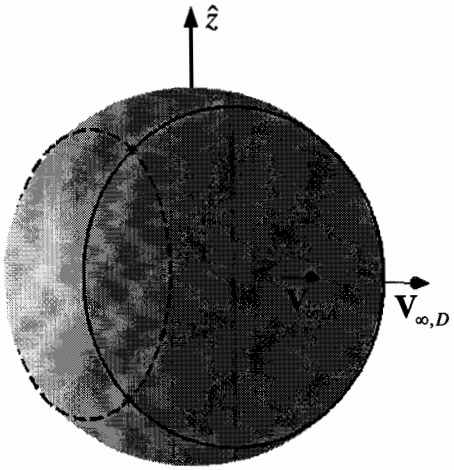

Figure 4 Loci of Periapses for Arrival (Solid) and Departure (Dashed) Orbits. Their Intersections Denote Possible Apo-Twist Maneuvers.

If the planet provides just enough bending to reach $\mathbf{V}_{\infty,D}$, then the circles become tangent and no apo-twist is required ($\phi = 0°$). However, as $\mathbf{V}_{\infty,A}$ and $\mathbf{V}_{\infty,D}$ become aligned (i.e. as $\alpha' \to 0°$) the circles will not intersect and no apo-twists may occur. Similarly, as $\alpha' \to 180°$ the circles will again become tangent at some point. In this case $\mathbf{V}_{apo}$ must be totally reversed, requiring the largest apo-twist maneuver ($\phi = 180°$). These special cases set the bounds on α' [Eq. (14)].

$$A_A + A_D \le \alpha' \le 180° - |A_D - A_A| \tag{14}$$

These bounds may also be verified by setting $\phi = 0°$ or $\phi = 180°$ in Eq.(13). Thus, when α' is too small or too large the apo-twist will not work (if no perturbations are present).

Perturbed Orbit Model: Solution Algorithm

The process of calculating apo-twist maneuvers when orbit perturbations are present is similar to the no perturbation case – determine the conditions necessary for the arrival orbit and departure orbit to have the same apoapsis vector, then calculate the angle (ϕ) between these orbits. The main difference is that the time when the maneuver is performed (just after arrival, just before departure, or any time in between) provides an extra degree of freedom in the apo-twist solution. Because of the added complexity of including precession effects, we adopted a numerical approach to the problem. Our method is generalized by the following steps:

1) Calculate the set of arrival and departure orbits where a tangential periapsis burn is possible via Eq. (3) by varying β_A and β_D.

2) Determine the precession of the arrival orbits up to a given maneuver time with an appropriate perturbation model. Similarly, reverse the precession of the departure orbits from departure time to the maneuver time.
3) Select combinations of β_A and β_D such that the three components of the apoapsis vector are close.
4) Use these β_A, β_D combinations as a starting point to drive the difference in arrival and departure apoapsis position components to zero via a non-linear equation solver.
5) Repeat 2-4 for different maneuver times until the parking orbit duration is sufficiently sampled.

We choose a relatively simple perturbation model that includes only the secular changes in the ascending node (Ω) and argument of periapsis(ω) due to oblateness (J_2) and the Sun and Moon. The corresponding angular rates are provided[11] in Eqs. (15) - (18).

$$\dot{\Omega}_{J_2} = -\frac{3}{2} n \frac{J_2 R_P^2}{a^2 \left(1-e^2\right)^2} \cos i \tag{15}$$

$$\dot{\omega}_{J_2} = \frac{3}{4} n \frac{J_2 R_P^2}{a^2 \left(1-e^2\right)^2} \left(4 - 5\sin^2 i\right) \tag{16}$$

$$\dot{\Omega}_{3B} = -\frac{1}{f}\frac{3}{16}\frac{n_{3B}^2}{n}\frac{\left(2+3e^2\right)\cos i}{\sqrt{1-e^2}}\left(3\cos^2 i_{3B} - 1\right) \tag{17}$$

$$\dot{\omega}_{3B} = \frac{1}{f}\frac{3}{16}\frac{n_{3B}^2}{n}\frac{\left(4-5\sin^2 i+e^2\right)}{\sqrt{1-e^2}}\left(3\cos^2 i_{3B} - 1\right) \tag{18}$$

In Eqs. (17) and (18) $f = 1$ for solar perturbations and $f = m_{\text{Earth}}/m_{\text{Moon}} \approx 81.3$ for lunar perturbations. Mars' moons were not included in the perturbation analysis. We choose this model because it captures the main perturbation effects on large, elliptical orbits. A more accurate model would include a higher order gravity field and variations in eccentricity and inclination. However, these effects are quite small compared to Eqs. (15) - (18) and were omitted to save computation time.

The added complexity of finding combinations of β_A and β_D for an apo-twist with perturbations is apparent in Figure 5. Now, the circles from Figure 4 have perturbed into intricate curves and several apo-twist locations (crossings) are possible instead of only two. Moreover, because the perturbations can move the apoapsis position significantly during the course of the stay time, the restrictions from Eq. (14) often no longer apply, especially for long stay times (e.g. 500 days). So, cases where the apo-twist is not possible without perturbations, may become possible when perturbations are present.

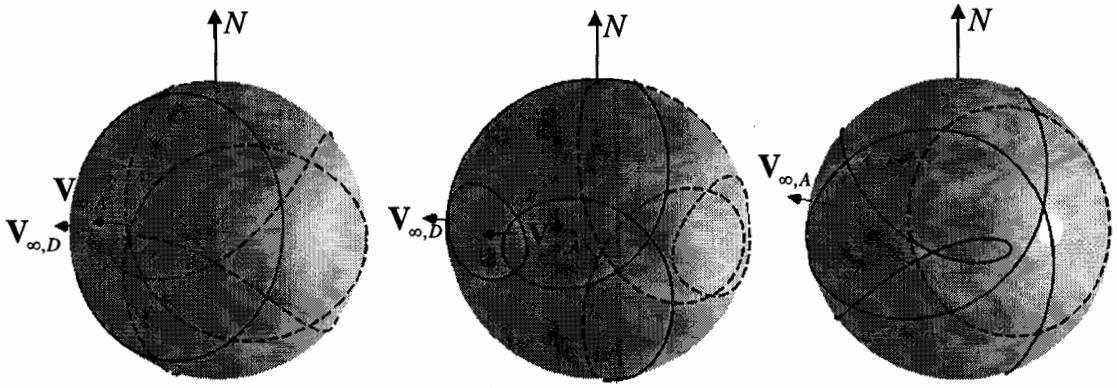

a) Arrival b) Middle of stay time c) Departure

Figure 5 Loci of Periapses for Perturbed Parking Orbits. Arrival is Solid, Departure is Dashed. N Denotes North Pole.

APPLICATION OF THE APO-TWIST

We now examine several current Mars mission scenarios to determine the effectiveness of the apo-twist. Specifically, we examine 1) stop-over cyclers,[4] which use a parking orbit at both Earth and Mars, 2) semi-cyclers,[2] which have a parking orbit at Mars and flyby Earth without stopping, and 3) fast-transfer conjunction trajectories,[12] which have low departure V_∞ and higher arrival V_∞ (for aerocapture) with relatively short (4-7 month) transfers. The fast-transfer conjunction trajectories are similar to those proposed for NASA's DRM.[1] All of these scenarios allow long stay times (500-700 days). The parking orbit is assumed to have a period of one day and a periapsis altitude of 300 km. A parking orbit of this size and shape allows a relatively small burn at periapsis, and still stays well within the sphere of influence of both Mars and Earth.

The ΔV and inclination drive the cost of the parking orbit. The ΔV indicates how much propellant is required to enter and depart the orbit, and the inclination determines how much propellant is needed to reach the surface. The inclination should be as close to the latitude of the launch/landing site as possible to make full use of the planet's rotation. But, the arrival inclination is not as important because the atmosphere may be used to reach the landing site with modest propellant expenditure (as long as the inclination is greater than the latitude of the site). If the mission involves rendezvous with a moon, then the parking orbit inclination should be as close to the moon's inclination as possible. However, in many scenarios the interplanetary transport vehicle is much more massive then the launch/landing vehicle, so the ΔV is usually weighted more than the inclination when minimizing propellant cost. Generally, low ΔV and prograde inclinations are desired, but the best combination is mission dependent.

To further assess the effectiveness of the apo-twist (which requires three burns) we compare it to a two-burn scheme. The first burn is the orbit insertion maneuver, which is performed tangentially to the velocity at periapsis. Thus, the insertion maneuver

may be replaced by atmospheric braking (aerocapture) if desired. The second burn is the departure maneuver. Generally, this is a three-dimensional maneuver (*not* tangential at periapsis) because the parking orbit and $\mathbf{V}_{\infty,D}$ are not perfectly aligned (Case 2, Figure 1). However, the departure ΔV may be minimized by proper selection of inclination and departure true anomaly.[7] Because the direction of $\mathbf{V}_{\infty,D}$ is included, this departure ΔV will always be greater than or equal to the tangential periapsis ΔV, which only includes the magnitude of $\mathbf{V}_{\infty,D}$ [Eq. (1)]. We measure the cost of the two-burn method as this extra ΔV required to account for the direction of $\mathbf{V}_{\infty,D}$ (i.e. the two-burn ΔV plus the tangential periapsis ΔV is the total ΔV required to reach the departure trajectory with the two-burn method). Like the apo-twist ΔV, this value provides the additional cost of including the relative geometry between the parking orbit and interplanetary trajectories.

The minimum ΔV and corresponding inclination, using both the apo-twist and two-burn methods, are provided in Tables 1 through 5. We calculate the heliocentric trajectories using a point-to-point conic solution between Earth and Mars. The resulting velocities relative to the planet then provide $\mathbf{V}_{\infty,A}$ and $\mathbf{V}_{\infty,D}$. The ΔV_A and ΔV_D columns give the cost of arriving and departing the 1 day × 300 km orbit with a tangential periapsis burn using Eq. (1). We note that in the case of aerocapture the propulsive $\Delta V_A \approx 0$. The ΔV_{add} columns under "Apo-twist" and "Two-burn" provide the additional cost of achieving the correct direction at departure for these methods. Thus the total cost is

$$\Delta V_{total} = \Delta V_A + \Delta V_D + \Delta V_{add} \tag{19}$$

Since the reorientation cost is a significant fraction of the total ΔV, it cannot be neglected in mission design. Moreover, an economical way of reducing this reorientation ΔV will lower the propellant cost of the mission.

Table 1
STOP-OVER CYCLER,[4] MARS

		Ideal		Apo-twist			Two-burn	
Arrival Date	Stay time (days)	ΔV_A (km/s)	ΔV_D (km/s)	i_A (deg)	i_D (deg)	ΔV_{add} (km/s)	i (deg)	ΔV_{add} (km/s)
7/13/2012	508	1.87	1.53	22.2	50.9	0.245	30.1	0.564
8/19/2014	513	1.74	1.01	154.8	142.5	0.104	150.8	0.181
10/5/2016	531	1.52	0.82	137.6	139.0	0.108	134.5	0.315
10/6/2018	592	2.03	1.38	140.5	138.8	0.027	141.7	0.061
2/20/2021	521	0.88	1.63	146.1	144.5	0.031	145.7	0.035

Table 2
STOP-OVER CYCLER,[4] EARTH

		Ideal		Apo-twist			Two-burn	
Arrival Date	Stay time (days)	ΔV_A (km/s)	ΔV_D (km/s)	i_A (deg)	i_D (deg)	ΔV_{add} (km/s)	i (deg)	ΔV_{add} (km/s)
7/1/2014	617	1.39	1.01	30.2	50.2	0.607	36.3	1.273
8/11/2016	637	1.22	0.88	140.7	140.4	0.336	136.9	0.795
10/16/2018	648	0.89	1.06	119.2	104.4	0.234	115.9	0.141
12/17/2020	640	0.96	1.32	117.8	68.5	0.752	94.2	1.698
2/21/2023	615	1.05	1.40	26.3	40.3	0.401	33.1	0.979

Table 3
VERSION II SEMI-CYCLER,[2] MARS

		Ideal		Apo-twist			Two-burn	
Arrival Date	Stay time (days)	ΔV_A (km/s)	ΔV_D (km/s)	i_A (deg)	i_D (deg)	ΔV_{add} (km/s)	i (deg)	ΔV_{add} (km/s)
8/2/2010	417	0.88	1.17	134.9	42.1	0.687	36.7	0.797
7/20/2012	499	1.64	1.66	140.9	60.0	0.604	41.1	1.233
7/16/2014	585	3.24	1.59	155.2	140.7	0.125	151.1	0.290
8/18/2016	615	3.08	1.22	144.1	131.5	0.110	140.4	0.266
10/12/2018	667	2.06	3.18	138.0	126.7	0.093	136.7	0.187

Table 4
FAST-TRANSFER CONJUNCTION-CLASS,[12] MARS

		Ideal		Apo-twist			Two-burn	
Arrival Date	Stay time (days)	ΔV_A (km/s)	ΔV_D (km/s)	i_A (deg)	i_D (deg)	ΔV_{add} (km/s)	i (deg)	ΔV_{add} (km/s)
6/1/2012	512	3.76	0.99	157.2	113.7	0.404	149.3	0.712
7/1/2014	555	3.88	1.08	156.5	151.1	0.045	154.5	0.032
7/31/2014	635	3.82	1.71	150.8	172.3	0.189	4.8	0.258
9/13/2018	666	3.95	2.19	145.1	159.4	0.123	150.1	0.332
11/21/2020	630	3.12	2.20	164.2	150.4	0.113	157.8	0.312

Table 5
FAST-TRANSFER CONJUNCTION-CLASS,[12] EARTH

		Ideal		Apo-twist			Two-burn	
Arrival Date	Stay time (days)	ΔV_A (km/s)	ΔV_D (km/s)	i_A (deg)	i_D (deg)	ΔV_{add} (km/s)	i (deg)	ΔV_{add} (km/s)
6/3/2014	639	2.50	0.95	22.2	42.2	0.351	27.9	0.486
7/5/2016	700	2.75	1.53	151.4	145.6	0.105	147.6	0.167
8/25/2018	680	2.69	1.48	147.4	145.8	0.225	141.6	1.064
11/7/2020	668	2.45	1.31	153.6	136.2	0.351	147.8	0.771
1/10/2023	641	2.78	1.29	156.5	109.2	0.733	148.4	1.460

The apo-twist ΔV is lower than the two-burn ΔV for almost all of the provided missions, which suggests that the apo-twist is more economical than the two-burn method. Moreover, the ΔV optimal inclinations for both methods are similar, so the two-burn scheme offers no apparent savings for surface or lunar rendezvous over the apo-twist.

If a larger period orbit is used (say, seven days instead of one) then the optimal arrival and departure ΔV's decrease, as does the velocity at apoapsis. Because V_{apo} is reduced, the apo-twist ΔV is generally smaller for longer period orbits. Also, since the velocity at periapsis increases for larger orbits, the average two-burn ΔV rises, countering the effect of using a "loose" parking orbit. In fact, as the parking orbit period approaches infinity (the parabolic case) the apo-twist ΔV_{add} goes to zero, but the two-burn ΔV_{add} does not. Consequently, increasing the orbit period will almost always decrease the total ΔV with the apo-twist, while the two-burn method may actually gain ΔV.

One notable drawback to increasing the size of the parking orbit is that there are fewer opportunities to perform the apo-twist maneuver. This effect is more pronounced at Mars than at Earth because the solar and lunar perturbations begin to dominate the decreasing J_2 effects as the size of the orbit increases. In fact, if a seven-day orbit is used for the June 1, 2012 Mars conjunction-class mission (Table 4) then no apo-twist maneuvers are possible. In this case, the apo-twist can be used in conjunction with the two-burn scheme to reduce total mission ΔV. There are also fewer arrival and departure apoapsis crossings if the stay time is relatively short (e.g. one month); however, for long stay times (500-700 days), an apo-twist maneuver is almost always possible.

Figures 6 and 7 provide a sampling of the apo-twist ΔV's and departure inclinations for the stop-over cyclers at Mars and Earth, respectively (see Tables 1 and 2). The arrival inclination is omitted because there is insignificant propellant cost associated with it for aerobraking missions. These figures are particularly useful in examining the trade between ΔV and inclination. For example, arrival date "4" in Figure 6 has a very low ΔV (0.03 km/s) apo-twist with an inclination of about 140°. However, if a prograde inclination is highly desired then an apo-twist with an inclination of 40° and ΔV of 0.75 km/s is possible for that arrival date. Since there are many different possible apo-twist maneuvers over the stay time, there is some freedom in the choice of ΔV and inclination for a given mission.

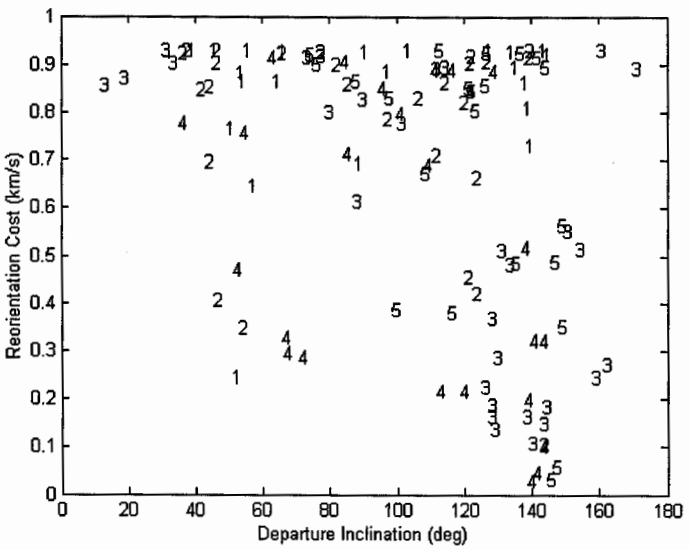

Figure 6 Apo-Twist ΔV and Departure Inclination for Mars Stop-Over Cyclers. Numbers 1-5 Correspond to the Five Arrival Dates in Table 1.

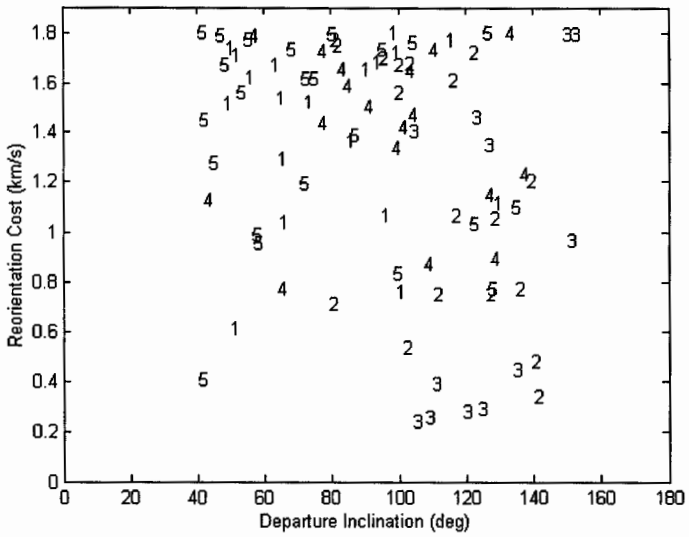

Figure 7 Apo-Twist ΔV and Departure Inclination for Earth Stop-Over Cyclers. Numbers 1-5 Correspond to the Five Arrival Dates in Table 2.

We note that arrival dates 1, 2, and 4 in Figure 6 and dates 1, 2, 4, and 5 in Figure 7 provide relatively low ΔV apo-twists with prograde departure inclinations (bottom-left quadrant of either graph). Though the ΔV's may be higher than the absolute minimum values found in Tables 1 and 2, these maneuvers may be preferred because they reduce the propulsion requirements of the launch vehicle. Also, multiple apo-twists may provide an economical means of attaining a desired inclination over the stay time. For example,

an apo-twist at arrival could rotate the trajectory to an equatorial orbit, then another apo-twist at departure would reorient the parking orbit for a tangential burn at periapsis on the return leg. This method could be an interesting extension of the single apo-twist maneuver. Another extension of the apo-twist is the "low-thrust apo-twist," where the orbit would be reoriented over the stay time via low-thrust propulsion (near apoapsis) to allow coapsidal coplanar maneuvers at arrival and departure.

CONCLUSIONS

Many Mars mission proposals do not account for the actual geometry between the parking orbit and the interplanetary trajectories, and thus appreciably underestimate the cost of the mission. An effective way to allow tangential burns at periapsis *and* still achieve the correct departure direction is to "twist" the orbit about the line of apsides via a maneuver at apoapsis — the apo-twist maneuver. This method works very well for long period, highly elliptic parking orbits, which are already desired for many proposed missions. We also demonstrate how to harness the natural perturbations on the parking orbit to minimize propellant cost. Reorienting the orbit prior to departure with the apo-twist almost always requires less ΔV than performing a non-tangential maneuver at departure. Consequently, less propellant mass is required, providing a more economical method for the exploration of Mars.

ACKNOWLEDGMENTS

The first author's work has been sponsored in part by an Andrews Fellowship at Purdue University.

NOTATION

A	=	hyperbolic half turn angle, degrees
c	=	cosine
$\hat{\mathrm{h}}$	=	direction of angular momentum
n	=	mean motion, degrees/second
R_p	=	planetary radius, km
$\mathbf{r}_p$	=	periapsis position vector, km
s	=	sine
$\mathbf{V}_\infty$	=	hyperbolic excess velocity, km/s
$\mathbf{V}_{apo}$	=	velocity at apoapsis, km/s
α	=	right ascension of $\mathbf{V}_\infty$, degrees
α'	=	angle between arrival and departure $\mathbf{V}_\infty$, degrees
β	=	B-plane angle, degrees
δ	=	declination of $\mathbf{V}_\infty$, degrees
ΔV	=	instantaneous change in velocity, km/s
ϕ	=	rotation along line of apsides, degrees
μ	=	gravitational parameter km^3/s^2

Subscripts

3B = perturbing third body
A = arrival
add = additional cost to include transfer geometry
D = departure

REFERENCES

1. Hoffman, S. and Kaplan, D., eds., "Human Exploration of Mars: The Reference Mission of the NASA Mars Exploration Study Team," NASA SP 6107, 1997.
2. Aldrin, B., Byrnes, D., Jones, R., and Davis, H., "Evolutionary Space Transportation Plan for Mars Cycling Concepts," American Institute of Aeronautics and Astronautics, AIAA Paper 2001-4677, Albuquerque, NM, Aug. 2001.
3. Bishop, R. H., Byrnes, D. V., Newman, D. J., Carr, C. E., and Aldrin, B., "Earth-Mars Transportation Opportunities: Promising Options for Interplanetary Transportation," American Astronautical Society, AAS Paper 00-255, The Richard H. Battin Astrodynamics Conference, College Station, TX, Mar. 20-21, 2000.
4. Penzo, P., and Nock, K., "Earth-Mars Transportation Using Stop-Over Cyclers," AIAA Paper 2002-4424, AIAA/AAS Astrodynamics Specialist Conference, Monterey, CA, August 2-5 2002.
5. Niehoff, J., Friedlander, A., and McAdams, J., "Earth-Mars Transport Cycler Concepts," International Astronautical Federation, IAF Paper 91-438, International Astronautical Congress, Montreal, Canada, October 5-11, 1991.
6. Desai, P., Braun, R., and Powell, R., "Aspects of Parking Orbit Selection in a Manned Mars Mission," NASA TP-3256, December 1992.
7. Desai, P., and Bugulia, J., "Arrival and Departure Impulsive ΔV Determination for Precessing Mars Parking Orbits," *Journal of the Astronautical Sciences*, Vol. 41, No.1, January-March 1993, pp. 1-18.
8. Thibodeau III, J. R., "Use of Planetary Oblateness for Parking-Orbit Alignment," NASA TN D-4657, July 1968.
9. Desai, P., and Bugulia, J., "Determining Mars Parking Orbits that Ensure Tangential Periapsis Burns at Arrival and Departure," *Journal of Spacecraft and Rockets*, Vol. 30, No. 4, July-August 1993, pp. 414-419.
10. Luidens, R. W., and Miller, B. A., "Efficient Planetary Parking Orbits with Examples for Mars," NASA TN D-3220, January 1966.
11. Chao, C. C., "An Analytic Integration of the Averaged Equations of Variation Due to Sun-Moon Perturbations and Its Application," AAS Paper 79-134, AAS/AIAA Astrodynamics Specialist Conference, Provincetown, MA, June 25-27, 1979.
12. Soldner, J. K., "Round Trip Mars Trajectories: New Variations on Classic Mission Profiles," AIAA Paper 90-3794, Aug. 1990.